Large Pupils Predict Goal-driven Eye Movements (supplementary material)

Sebastiaan Mathôt[1], Alisha Siebold[2,3], Mieke Donk[2], and Françoise Vitu[1]

[1] Aix-Marseille University, CNRS, LPC UMR 7290, Marseille, France

[2] Dept. of Cognitive Psychology, VU University Amsterdam

[3] Center for Mind/Brain Sciences, University of Trento, Italy

Address for correspondence:

Aix-Marseille University, CNRS

Laboratoire de Psychologie Cognitive, UMR 7290

3 Place Victor Hugo

Centre St. Charles, Bâtiment 9, Case D

13331 Marseille

France

Overview

Materials and availability

All experimental materials, where possible given license restrictions, are available from https://github.com/smathot/materials_for_P0010.5.

Linear mixed-effects models

The procedure used to construct the linear mixed-effects models (LME) is described in the main text. Models were estimated using the `lmer()` function from the `lme4` (v1.0, Bates et al., 2014) package for R (v3.0.2). In all models reported below, fixation saliency is the dependent variable, using the units provided by the saliency-map algorithm (range: 0-255). The reference value for continuous variables is 0.

Table 1

The LME for Exp. 1 used to estimate the partial slope of the relationship between pupil size and fixation saliency. Based on an LME model with by-participant random intercept and random slope for pupil size.

Fixed effect	***β***	***SE***	***t***
(Intercept)	33.7178	1.1174	30.1763
Trial nr.	0.0043	0.0026	1.6627
Fix nr.	-0.0430	0.0078	-5.4885
Luminance	-4.4245	0.6704	-6.5995
Eccentricity	-0.0143	0.0008	-17.8365
Horiz. gaze pos.	-0.0018	0.0004	-4.9622
Vert. gaze pos.	-0.0130	0.0005	-25.7356
Fix. dur.	0.0032	0.0014	2.3817
Sacc. size	-0.0045	0.0007	-6.2162
Pupil size	2.6798	0.4520	5.9283

Table 2

The LME for Exp. 2 used to estimate the partial slope of the relationship between pupil size and fixation saliency. Based on an LME model with by-participant random intercept and random slope for pupil size.

Fixed effect	***β***	***SE***	***t***
(Intercept)	21.1283	0.6482	32.5945
Trial nr.	-0.0200	0.0041	-4.8428
Fix nr.	-0.0340	0.0093	-3.6508
Luminance	8.9277	0.6233	14.3223
Eccentricity	-0.0114	0.0009	-13.0753
Horiz. gaze pos.	0.0002	0.0004	0.5431
Vert. gaze pos.	-0.0119	0.0006	-20.2975
Sacc. size	-0.0036	0.0007	-4.8078
Pupil size	1.5585	0.4819	3.2341

Table 3

The LME for Exp. 2, including effects of stimulus type, task instruction, and relevant interaction terms. Fractals are used as reference stimulus type. Free-viewing is used as reference task instruction. Based on an LME model with by-participant random intercept and random slopes for pupil size, instruction, and stimulus type.

Fixed effect	***β***	***SE***	***t***
(Intercept)	20.4169	0.6155	33.1686
Trial nr.	-0.0201	0.0041	-4.8953
Fix. nr.	-0.0320	0.0093	-3.4293
Luminance	9.4253	0.6371	14.7940
Eccentricity	-0.0116	0.0009	-13.2442
Horiz. gaze pos.	0.0002	0.0004	0.4105
Vert. gaze pos.	-0.0119	0.0006	-20.1384
Sacc. size	-0.0036	0.0007	-4.7724
Pupil size	0.4181	0.7254	0.5763
Instruction (memory)	1.3836	0.7401	1.8695
Instruction (search)	-1.1170	13.4215	-0.0832
Stim. type (scene)	0.2630	0.3914	0.6721
Pupil size x Instruction (memory)	-0.3526	0.9916	-0.3556
Pupil size x Instruction (search)	2.3634	1.0171	2.3237
Pupil size x Stim. type (scene)	1.2715	0.2783	4.5694

Table 4

The LME for Exp. 3, including the effects of condition and condition x pupil size interaction. Dual task is used as reference condition. Based on an LME model with by-participant random intercept and random slopes for pupil size and condition.

Fixed effect	***β***	***SE***	***t***
(Intercept)	31.6644	0.6421	49.3176
Trial nr.	0.0114	0.0021	5.4130
Sacc nr.	-0.0419	0.0032	-13.1083
Luminance	-5.3864	0.3108	-17.3280
Eccentricity	-0.0141	0.0004	-39.2549
Horiz. gaze pos.	-0.0042	0.0002	-23.4865
Vert. gaze pos.	-0.0129	0.0002	-53.8011
Fix. dur.	0.0082	0.0006	13.2268
Sacc. size	-0.0028	0.0003	-8.7236
Pupil size	0.5167	0.3381	1.5282
Condition (single)	-0.1532	8.9177	-0.0172
Pupil size x Condition (single)	0.4315	0.1769	2.4392

Pupil-size transformations

Table 5 lists the log-likelihood values of the LME models for different pupil-size transformations. High (i.e. less negative) log-likelihood values are better. The model shown in Table 1 corresponds to the D^{-1} model. Strikingly, transformations that reduce positive skewness work better than transformations that introduce positive skewness. Pupil-size area (D^2), which we and others have frequently used as dependent measure (Mathôt, Dalmaijer, Grainger, & Van der Stigchel, 2014; Mathôt, van der Linden, Grainger, & Vitu, 2013, 2015), is clearly suboptimal, at least for the present purpose.

Table 5

Log-likelihood values of LME models with different pupil-size transformations.

Transformation	**Log-likelihood**
D^{-1}	-293956.7423
log(D)	-293957.1798
$D^{0.5}$	-293958.2633
D	-293959.7822
D^2	-293974.1862
D^3	-293996.3642

Relationship between luminance and saliency

It is well known that luminance is the primary determinant of pupil size (e.g., Ellis, 1981): The pupil constricts when looking at, or even attending to (Binda, Pereverzeva, & Murray, 2013; Mathôt et al., 2013), bright surfaces. Therefore, if luminance were consistently and positively correlated with visual saliency, and if this were not controlled for, a pupillary light response might fully explain our results. Our primary way to control for this potential confound is by estimating pupillary luminance maps, and entering values from these maps as control predictor into the models, as described above and in the main text.

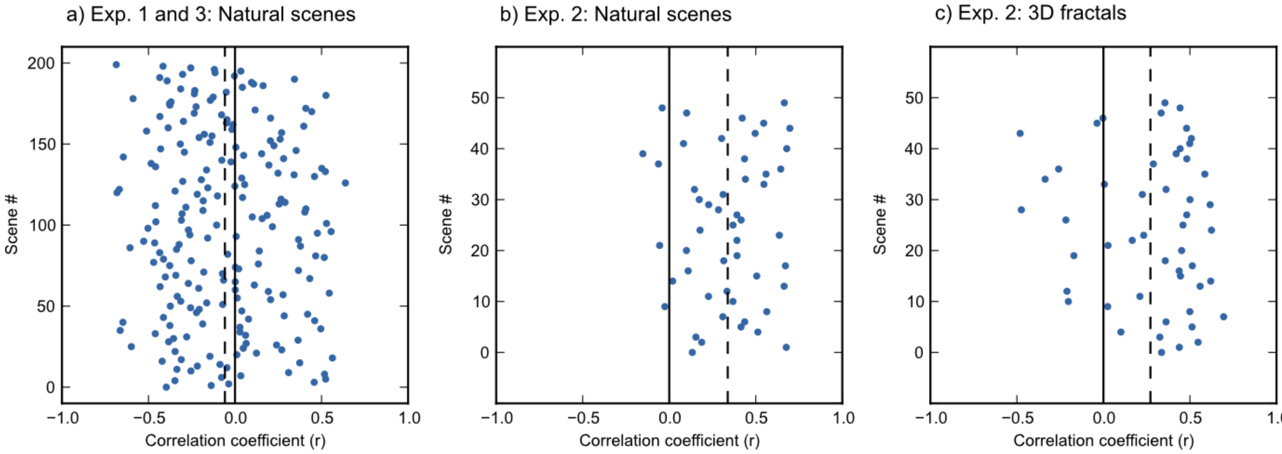

Figure 1. *The correlation between visual saliency and luminance. Dots correspond to individual images. a) The 200 images used for Exp. 1 and 3. b) The 50 natural scenes used for Exp. 2. c) The 50 3D fractals used for Exp. 2.*

However, it is also informative to directly consider the relation between luminance and saliency, in order to dispel any lingering suspicion that this may have confounded our results. As can be seen in Figure 1 (see also the factor 'Fixation luminance' in Tables 1-3), the direction of this correlation varies widely from image to image, and also between the different image sets. (The values on the x-axis indicate the correlation coefficient between saliency and luminance values for the same pixel, separately for each image.) For the photos from the UPenn natural image database (Tkačik et al., 2011), there was a weak negative correlation (a two-sided one-sample t-test against 0 on the correlation coefficients for each image: $M = -.059$, $SE = .023$, $t(199) = 2.580$, $p = .011$). This may reflect the fact that the primary source of brightness in the savanna is the sky, which is not very salient. For the images from the Campus Scene collection (Burge & Geisler, 2011), there was a moderate positive correlation ($M = .338$, $SE = 0.032$, $t(49) = 10.420$, $p < .001$). This presumably reflects the fact that these images were taken in an urbanized environment, where bright lights are a dominant source of saliency. For the 3D Mandelbulber-generated fractals (Marczak, 2012), there was also a moderate positive correlation ($M = 0.272$, $SE = 0.043$, $t(49) = 6.259$, $p < 0.001$), presumably due to the use of virtual light sources.

For our purpose, the crucial point to note is that the correlation between saliency and brightness is variable, and can be positive or negative depending on the specifics of the stimuli.

However, the correlation between pupil size and saliency is invariably negative (or positive when using an inverse transformation), and can therefore not be (fully) related to brightness.

Acknowledgements

The research leading to these results has received funding from the People Programme (Marie Curie Actions) of the European Union's Seventh Framework Programme (FP7/2007-2013) under REA grant agreement n° 622738.

References

Bates, D., Maechler, M., Bolker, B., Walker, S., Christensen, R. H. B., & Singmann, H. (2014). *lme4: Linear mixed-effects models using Eigen and S4*. Retrieved from http://cran.r-project.org/web/packages/lme4/index.html

Binda, P., Pereverzeva, M., & Murray, S. O. (2013). Attention to bright surfaces enhances the pupillary light reflex. *Journal of Neuroscience*, *33*(5), 2199–2204. doi:10.1523/JNEUROSCI.3440-12.2013

Burge, J., & Geisler, W. S. (2011). Optimal defocus estimation in individual natural images. *Proceedings of the National Academy of Sciences*, *108*(40), 16849–16854. doi:10.1073/pnas.1108491108

Ellis, C. J. (1981). The pupillary light reflex in normal subjects. *British Journal of Ophthalmology*, *65*(11), 754–759. doi:10.1136/bjo.65.11.754

Marczak, K. (2012). *Mandelbulber*. Retrieved from http://mandelbulber.com/

Mathôt, S., Dalmaijer, E., Grainger, J., & Van der Stigchel, S. (2014). The pupillary light response reflects exogenous attention and inhibition of return. *Journal of Vision*, *14*(14), 7. doi:10.1167/14.14.7

Mathôt, S., van der Linden, L., Grainger, J., & Vitu, F. (2013). The pupillary response to light reflects the focus of covert visual attention. *PLoS ONE*, *8*(10), e78168. doi:10.1371/journal.pone.0078168

Mathôt, S., van der Linden, L., Grainger, J., & Vitu, F. (2015). The pupillary light response reflects eye-movement preparation. *Journal of Experimental Psychology: Human Perception and Performance*, *41*(1), 28–35. doi:10.1037/a0038653

Tkačik, G., Garrigan, P., Ratliff, C., Milčinski, G., Klein, J. M., Seyfarth, L. H., … Balasubramanian, V. (2011). Natural images from the birthplace of the human eye. *PLoS ONE*, *6*(6), e20409. doi:10.1371/journal.pone.0020409